Organic Electronics 13 (2012) 491–497

Contents lists available at SciVerse ScienceDirect

Organic Electronics

journal homepage: www.elsevier.com/locate/orgel

# Thin ferroelectric poly(vinylidene fluoride-chlorotrifluoro ethylene) films for thermal history independent non-volatile polymer memory

Richard Hahnkee Kim, Seok Ju Kang, Insung Bae, Yeon Sik Choi, Youn Jung Park, Cheolmin Park *

*Department of Materials Science and Engineering, Yonsei University, Seoul, Republic of Korea*

ARTICLE INFO

*Article history:*
Received 4 October 2011
Received in revised form 18 November 2011
Accepted 19 November 2011
Available online 21 December 2011

*Keywords:*
Ferroelectric polymer
Poly(vinylidene fluoride-chlorotrifluoro ethylene)
Crystal phase
Remnant polarization
Non-volatile polymer memory
Ferroelectric capacitor

ABSTRACT

In this study, we investigated the molecular and microstructures of thin poly(vinylidene fluoride-chlorotrifluoro ethylene) (PVDF-CTFE) copolymer films with three different CTFE compositions of 10, 15, 20 wt% with respect to PVDF in relation with their ferroelectric properties. All PVDF-CTFE annealed at 130 °C showed consecutive *TTTT* trans conformation with β type crystals while films molten and re-crystallized from a temperature above their melting points exhibited α type crystals with characteristic *TGTG* conformation. Microstructures of the films treated with the two different thermal histories also supported the formation of β and α type crystals with hundreds of nanometer scale sphere caps and micron level spherulites, respectively. Interestingly, PVDF-CTFE films with both α and β type crystals gave rise to relatively high remnant polarization of approximately 4 $\mu C/cm^2$ in metal/ferroelectric/metal capacitors regardless of the composition of CTFE. The ferroelectric polarization of a PVDF-CTFE film independent of thermal processing history allowed a wide processing window and easy fabrication protocol, resulting in a non-volatile ferroelectric field effect transistor memory which exhibited saturated hysteresis loops with the current ON/OFF ratio of approximately $10^3$ at ±60 V sweep and reliable data retention.



## 1. Introduction

Ferroelectric polarization is an attractive property as the mechanism for non-volatile switching of tremendously demanding memory devices because the bistable polarization arising from ferroelectricity can be used as two binary states of a memory element. Work on ferroelectric memories has recently extended into the commercial development of inexpensive memory cards, integrating ferro electric ceramic crystal films such as lead zirconate titanate (PZT) into the gate insulator of field-effect transistors (FETs) [1,2]. There are also representative ferroelectric polymers such as poly(vinylidene fluoride) (PVDF) and its copolymer poly(vinylidene fluoride-co-trifluoroethylene) (PVDF-TrFE), and these polymers have great benefits due to their excellent ferroelectric properties, easy and cost effective fabrication for large area applications [3–8]. In terms of device architecture, ferroelectric polymers have been employed to various memory units such as non-destructive ferroelectric field effect transistors (FeFETs) and destructive metal/ferroelectric/metal (MFM) capacitor [9–19].

Despite of the advantages of thin ferroelectric polymer films, there are several issues still remaining for applying them applying for non-volatile memories. For instance, although PVDF exhibits its maximum ferroelectric properties from the polar all-trans β crystalline phase [20], it often gives rise to characteristic α and γ form crystals with non-polar TGTG' and less-polar TTTG conformation, respectively. This requires additional processes to transform either α or γ into ferroelectric β form including mechanical stretching [21], electrical poling [22], crystallization under

* Corresponding author. Tel.: +82 2 2123 2833; fax: +82 2 312 5375.
*E-mail address:* cmpark@yonsei.ac.kr (C. Park).

1566-1199/$ - see front matter © 2011 Elsevier B.V. All rights reserved.
doi:10.1016/j.orgel.2011.11.018

high pressure [23]. In the case of PVDF-TrFE, on the other hand, the ferroelectric β phase is always developed regardless of processing methods because a F-atom with large steric hinderence substituted for H-atom in TrFE unit renders the trans conformation more favored than gauche one. PVDF-TrFE, however, still has a limitation of operating temperature with relatively low Curie temperature (~80 °C) compared with that of PVDF (~150 °C). Another issue is the alternation of molecular orientation depending upon thermal processing history of a PVDF-TrFE film and the consequent modification of its ferroelectric properties. For example, remnant polarization ($P_r$) value of a thin PVDF-TrFE film in MFM capacitor was in general maximized when the film was annealed around 135 °C, while significant reduction of $P_r$ occurred when a film is molten over 170 °C and subsequently re-crystallized [24,25]. The previous studies have demonstrated that the reduction of $P_r$ arises mainly from a preferred crystal orientation of the film which is ineffective for ferroelectric switching upon melting and recrystallization. It would be, therefore, beneficial if one can develop a new ferroelectric polymer with relatively constant $P_r$ regardless of thermal processing history as well as the types of its crystals.

Other fluorinated polymers such as poly(vinylidene fluoride-chlorotrifluoro ethylene) (PVDF-CTFE) and poly (vinylidene fluoride-hexafluoropropene) (PVDF-HFP) have been extensively studied, but many researches have been focused on the application for electrical energy storage [26–30]. Only a few have dealt with the relationship between the molecular and microstructure of PVDF-CTFE and the resulting ferroelectric properties. In particular, a recent work by Zhang and co-workers has pointed out that PVDF-CTFE prefers to be stabilized in α type phase having TGTG' conformations with a descent $P_r$ of approximately 4 μC/cm$^2$ [31]. Considering that PVDF and its copolymer with non-polar α crystals are paraelectric, making them not suitable for non-volatile memory applications, the observation by Zhang et al. greatly motivated us to investigate further details of molecular and microstructure of thin PVDF-CTFE films for potential non-volatile memory applications.

In this paper, we attempted to understand the relation between the molecular and microstructures of thin PVDF-CTFE films with three different CTFE compositions of 10, 15, 20 wt% with respect to PVDF and their ferroelectric properties for non-volatile polymer memory. For all PVDF-CTFEs investigated, the characteristic β and α type crystals were developed when a thin PVDF-CTFE film was annealed at 130 °C and re-crystallized from molten state at a temperature above the melting point (~160 °C), respectively. In spite of the different types of crystals of the samples dependent upon thermal processing histories, both films showed typical ferroelectric hysteresis loops with $P_r$ value of approximately 4 μC/cm$^2$ in MFM capacitors. Furthermore, a FeFET memory containing a thin PVDF-CTFE film with either α or β type crystals confirmed the unique ferroelectric properties of the film. The device exhibited a well-saturated source-drain current hysteresis loop with ON/OFF current ratio of approximately $10^3$ at gate voltage sweep of ±60 V and reliable non-volatile data retention.

## 2. Experimental sections

### 2.1. Materials and film preparation

The PVDF-CTFE copolymers with three different CTFE compositions of 10, 15, 20 wt% with respect to PVDF were purchased from Aldrich. The melting ($T_m$) and Curie ($T_c$) temperatures of PVDF-CTFE (90/10) measured with calorimetric measurements (Perkin-Elmer DSC-7) were 160 and 110 °C, respectively. 5 wt% PVDF-CTFE solutions in dimethylformamide (DMF) were spin-coated at a spin rate of 2000 rpm for 1minute in a nitrogen-filled box after filtration with 1 μm PTFE membrane on various electrode substrates such as Al, Au and highly boron-doped Si substrate. Some of the films were annealed on a Linkam 600 heating stage at 130 °C for 2 h and others were treated at 200 °C for 30 min and subsequently re-crystallized by slowly cooling the samples to room temperature. Thin PVDF-CTFE films were approximately 400 nm in thickness, confirmed by ellipsometry (SE MG1000-VIS spectroscopic ellipsometer).

### 2.2. Capacitor fabrication and characterization

Metal/PVDF-CTFE/metal capacitors were made with a highly boron-doped Si substrate as the bottom electrode. Aluminum top electrodes were thermally evaporated on polymer films using a shadow mask with holes 200 μm in diameter under a pressure of $10^{-6}$ mbar (1 mbar = 100 Pa) and an evaporation rate of 0.1 nm/s. Ferroelectric polarization-voltage measurements were performed using a virtual ground circuit (Radiant Technologies Precision LC unit).

### 2.3. FeFET fabrication and characterization

Fabrication of a FeFET memory with a single-crystal TIPS-PEN active channel began with the formation of a bilayered PVDF-CTFE/poly(4-vinylphenol)(PVP) gate dielectric consecutively spin-coated on a highly boron-doped Si gate electrode. Single-crystal TIPS-PEN was then deposited on the PVDF-CTFE layer by method as described previously [32]. In order to reduce the leakage current between the gate and drain electrodes of a FeFET memory, a thin PVP film was prepared from a 5wt% solution of PVP and poly(melamine-co-formaldehyde) in propylene glycol monomethyl ether acetate (PGMEA). The film was subsequently cross-linked by curing at 200 °C for 30 min. Square-shaped source and drain Au electrodes with the size and thickness of 200 μm and 80 nm, respectively, were thermally evaporated through a shadow mask on the TIPS-PEN single crystals randomly deposited on the PVDF-CTFE surface. A single crystalline TIPS-PEN firmly bridged between source and drain electrodes completed the fabrication of a bottom gate top contact FeFET memory. The electrical properties of the devices were recorded using semiconductor systems (E5270B, HP4284A, Agilent Technologies). All measurements were done in a metallic shielded box at room temperature in air.

### 2.4. Microstructure characterization

Tapping Mode Atomic force microscopy (TM-AFM) was performed in height contrast by a Digital Instrument

Nanoscope 3100 microscope. Optical microscopy (OM) (Olympus BX 51 M) was used to visualize single crystalline TIPS-PENs in the FeFET devices. 2D Grazing-Incidence X-ray Diffraction (GIXD) was performed on the 4C2 beam line at the Pohang Accelerator Laboratory in Korea (incidence angle: ~0.09–0.15°). The samples were mounted on an X and Y axes goniometer. Monochromatized X-rays ($\lambda$ = 0.1608 nm) under vacuum and the full range of available incidence angles were used. The scattered beam intensity was recorded with an SCX 4300-165/2 CCD detector (Princeton Instruments). Grazing incident reflection absorption spectra (GIRAS) were measured using a Bruker-IFS66 V spectrometer for analyzing the chain conformations of PVDF-CTFE layers.

## 3. Results and discussion

The GIRAS spectra in Fig. 1 revealed the chain conformations of thin PVDF-CTFE (90/10 and 85/15) films prepared with two different thermal histories: (1) annealed at 130 °C for 2 h and (2) re-crystallized from molten state. We also investigated the effect of metal substrates on the chain conformations of PVDF-CTFE films under the different thermal histories. In Fig. 1a, a PVDF-CTFE 90/10 film on Au substrate exhibits the strong IR absorption bands at 510, 840, 1280, and 1432 $cm^{-1}$ when either as-cast from the solution or annealed at 130 °C. These peaks are well-matched with the IR bands corresponding to consecutive TTTT conformation with typical ferroelectric β crystals of PVDF and PVDF-TrFE [33–37]. The β type crystals developed in an *as-cast* film became more prominent upon thermal annealing at 130 °C due to the enhanced degree of crystallization. As a film was molten at 200 °C and re-crystallized during slow cooling, the absorption peaks representing β crystals disappeared and new absorption ones at 490, 612 $cm^{-1}$ were significantly developed which corresponded to non-polar TGTG' conformation with α type crystals routinely observed in PVDF.

When Al substrate was employed, the similar chain conformations were also developed to those found on Au surface, depending upon the thermal history as shown in Fig. 1b. The β type crystals were formed in a PVDF-CTFE 90/10 film annealed at 130 °C while α crystals were preferentially developed when a film was molten and subsequently re-crystallized. It should be noted that Au surface is more efficient for producing β type crystals in a film annealed at 130 °C than Al one when relative absorption intensities of β type crystals on Au were carefully compared with those on Al in Fig. 1a and b. We have also observed the β type crystals of PVDF on Au surface more efficiently developed during rapid thermal annealing than on polar oxide surfaces such as $SiO_2$, and $Al_2O_3$ [38]. Other PVDF-CTFE 85/15 and PVDF-CTFE 80/20 films deposited on both Au and Al substrate also exhibited characteristic β and α type crystals when the samples were annealed at 130 °C

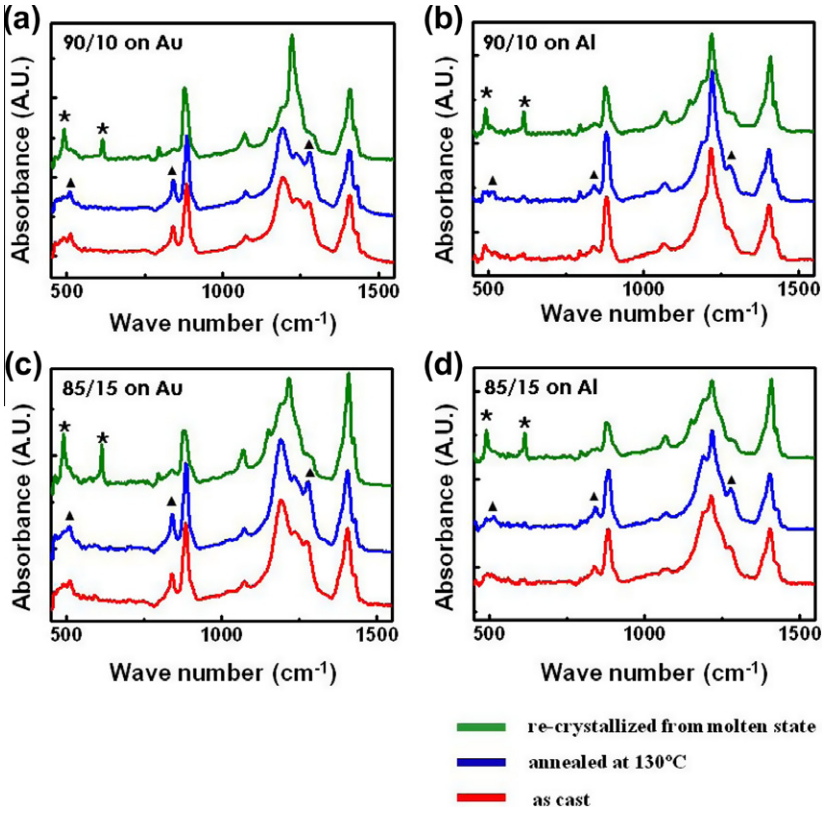


**Fig. 1.** GIRAS spectra of PVDF-CTFE 90/10 films spin coated on (a) Au and (b) Al substrate with various thermal processing histories. (c) and (d) show GIRAS spectra of PVDF-CTFE 85/15 films spin-coated on Au and Al substrate, respectively with various thermal processing histories.

and re-crystallized from molten state, respectively. Fig. 1c and d clearly show the β type crystals in a PVDF-CTFE 85/15 film formed during spin-coating were further developed during thermal annealing at 130 °C on both metal substrates. GIRAS results similar to Fig. 1c and d were also obtained for PVDF-CTFE 80/20 films (Supporting information, S1).

TM-AFM visualized the surface microstructures of PVDF-CTFE copolymer films experienced with the two different thermal histories as shown in Fig. 2a and b. A PVDF-CTFE 90/10 film annealed at 130 °C for 2 h on highly boron-doped Si substrate displayed the unique surface morphology with micron-sized bumps over the film which was very similar to ones of a thin PVDF film with the characteristic β crystals in our previous work [38]. A sample re-crystallized from molten state clearly shows well defined spherulitic edge-on lamellae of approximately 20 nm in width, reminiscent of the characteristic microstructure of α crystals of PVDF as shown in Fig. 2b [39]. Both PVDF-CTFE 85/15 and 80/20 also exhibited the surface microstructures similar to those of PVDF-CTFE 90/10 (Supporting information, S2).

The molecular structures of PVDF-CTFE films revealed by 2D GIXD confirmed the different polymorphic crystal formation dependent upon thermal processing history as shown in Fig. 2c and d (also see Supporting information, S3). A GIXD pattern of a PVDF-CTFE 90/10 annealed at 130 °C in Fig. 2c displays an intensified reflection at the scattering vector, $q_{xy}$ of approximately 12.8 $nm^{-1}$ arising from either (1 1 0) or (2 0 0) plane of an orthorhombic crystal cell in which the similar lattice spacing of (1 1 0) and (2 0 0) gives rise to a pseudo-hexagonal diffraction pattern. The results imply that one of the two planes is preferentially aligned perpendicular to the substrate with the polymer chains preferentially oriented parallel to the surface of Si substrate. On the other hand, a GIXD pattern of a PVDF-CTFE 90/10 film re-crystallized from molten state in Fig. 2d shows four intensified reflections matched with (0 2 0), (1 0 0), (1 1 0), and (0 2 1) planes of non-polar α type crystals of PVDF trans-crystallized from air surface [39]. In particular, the (0 2 0) reflection at meridian indicates that the *b* axis of the unit cell of the α crystals is oriented normal to the surface, resulting in edge-on crystalline lamellae as shown in Fig. 2b. Both TM-AFM and X-ray diffraction results of PVDF-CTFE 90/10 films which exhibited two different crystal polymorphs when treated in the different thermal histories are consistent with GIRAS ones. The similar molecular structures were observed in other PVDF-CTFE films with different CTFE compositions (Supporting information, S3).

In order to examine non-volatile switching of the PVDF-CTFE films, we investigated polarization (*P*) behaviors of those films as a function of applied electric voltage (*E*) in MFM capacitors. Fig. 3 shows *P*–*E* hysteresis loops of Al/PVDF-CTFE 90/10 /highly doped Si capacitors with different thermal histories. First of all, a MFM capacitor with an *as-cast* film also exhibits a hysteresis loop with $P_r$ of approximately 3.6 μC/$cm^2$ at the sweeping voltage of ±60 V in Fig. 3a. A capacitor with a film annealed at 130 °C displays a typical ferroelectric hysteresis loop nearly saturated with

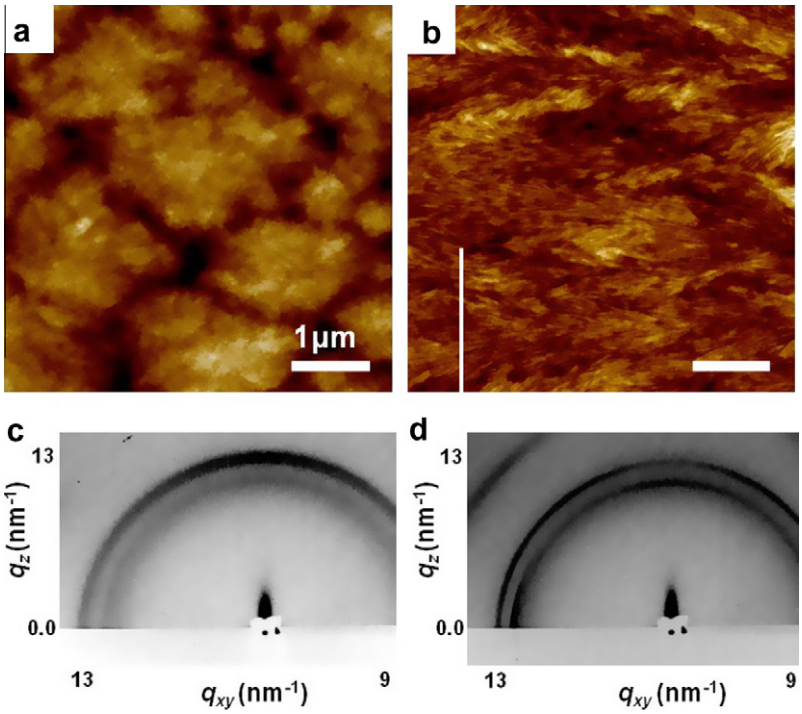


**Fig. 2.** TM-AFM images in height contrast of the surface microstructures of PVDF-CTFE 90/10 films (a) annealed at 130 °C for 2 h, and (b) re-crystallized from molten state at 200 °C. (c) and (d) show 2D GIXD patterns of thin PVDF-CTFE 90/10 films annealed at 130 °C and re-crystallized from molten state at 200 °C, respectively.

$P_r$ of approximately 4.2 μC/cm$^2$ slightly greater than that with the *as-cast* film at the voltage of ±60 V due to the enhanced β type crystals developed during the annealing as shown in Fig. 3b. There is relatively large polarization difference between the saturated polarization and $P_r$ which was attributed to non-ferroelectric amorphous regions as well as grain boundaries of the films [40].

A MFM capacitor containing a PVDF-CTFE film molten and subsequently re-crystallized also shows a nearly saturated hysteresis curve similar to one observed with a film annealed at 130 °C as shown in Fig. 3c. The averaged $P_r$ value and Coercive voltage ($E_c$) are also very similar to those with the film annealed at 130 °C as summarized in Table 1. It is apparent that in the case of PVDF-CTFE even α type crystals also exhibit non-volatile ferroelectric switching in MFM capacitors. The $P_r$ values similar with each other regardless of the type of polymorphic crystals in PVDF-CTFE films allowed a new non-volatile memory independent of thermal process history, making thermal budget for device fabrication greater than other conventional ferroelectric polymers such as PVDF and PVDF-TrFE. Other PVDF-CTFE films with different CTFE compositions also showed the ferroelectric hysteresis loops depending upon thermal treatment conditions similar to those with PVDF-CTFE 90/10 (Supporting information, S4). The ferroelectric performance of MFM capacitors with three PVDF-CTFE films examined is also summarized in Table 1.

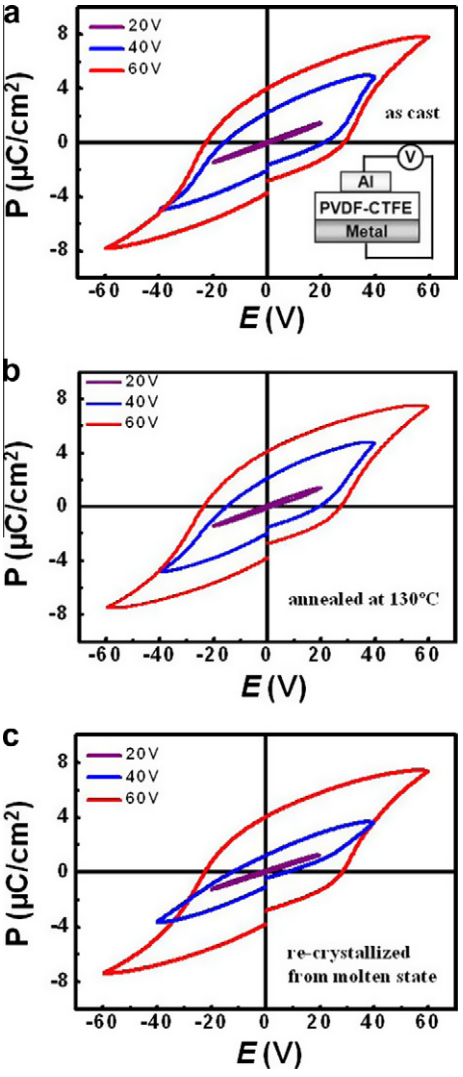


**Fig. 3.** Polarization ($P$) versus applied voltage ($V$) hysteresis loops of Al/PVDF-CTFE 90/10/highly-doped Si capacitors with thin ferroelectric films (a) as-cast, (b) annealed at 130 °C for 2 h and (c) re-crystallized from molten state at 200 °C. The inset of (a) represents a schematic of a MFM capacitor.

The unique ferroelectric properties of PVDF-CTFE independent of the type of polymorphic crystals also afforded facile fabrication of the reliable FeFET type non-volatile memory elements with thin PVDF-CTFE films free from thermal processing history. We employed a single crystalline TIPS-PEN active channel for non-destructive bistability in a FeFET. Ribbon shape single crystalline TIPS-PENs were well developed on a PVDF-CTFE 90/10 film deposited on a PVP insulating layer which was used to reduce gate current leakage as shown in Fig. 4a. A thin and flat single crystal of TIPS-PEN was bridged between source and drain electrode in a bottom gate and top contact FeFET schematically illustrated in Fig. 4b. A birefringent image of the single crystal under cross-polarizers also exhibits highly uniform and flat crystal nature in the inset of Fig. 4a. As demonstrated in our previous works, single crystalline TIPS-PEN gave rise to well saturated p-type current modulation with its field effect mobility of approximately 0.5 cm$^2$/Vs when fabricated into a conventional organic field effect transistor with 200 nm thick $SiO_2$ gate dielectric layer [32].

We prepared two types of FeFETs with ferroelectric PVDF-CTFE 90/10 films with β and α type crystals by employing the different thermal processing histories: (1) annealed at 130 °C and (2) re-crystallized from the molten state, respectively. The drain current ($-I_{DS}$) versus gate voltage ($V_G$) curve scanned with the sweep voltage of ±60 V at a fixed $V_{SD}$ of −5 V shown in Fig. 4b clearly displays a typical ferroelectric hysteresis with the drain current ON/OFF bistability ratio of $10^3$ at zero gate bias in a FeFET with a PVDF-CTFE film annealed at 130 °C. The hysteresis curves are varied in both memory window and ON current, which tend to increase with gate voltage. The curves are saturated when the gate voltage was applied above ±60 V. The sharp increase of $I_{SD}$ with negative gate voltage arose from excess holes accumulated in the TIPS-PEN single crystal at the interface with PVDF-CTFE film. Furthermore, when the gate voltage went back to zero, $I_{SD}$ remained at the value saturated with the gate voltage of −60 V due to the non-volatile H-F dipoles in the ferroelectric PVDF-CTFE film. The subsequent positive gate voltage on the device reversed the H-F dipoles with H atoms pointing to the TIPS-PEN layer, resulting in a rapid decrease of $I_{SD}$. The non-volatility of polarization again made the current remaining same even after removal of positive voltage. As described in the previous works [3,18], the surface charge density of approximately 4 μC/cm$^2$ on the ferroelectric PVDF-CTFE layer is still sufficient to fully accumulate counter charges in the organic semi-conductor at the channel and the ferroelectric layer interface, leading to a fully saturated source-drain current hysteresis curve as shown in Fig. 4b.

**Table 1**
Ferroelectric properties of MFM capacitors with PVDF-CTFE films with three different CTFE compositions prepared with various thermal processing steps.

| Sample | PVDF:CTFE (wt%) | As-cast | | Annealed at 130 °C for 2 h | | Molten and re-crystallized | |
|---|---|---|---|---|---|---|---|
| | | $P_r$ (μC/cm$^2$)* | $\Delta E_C$ (V)* | $P_r$ (μC/cm$^2$)* | $\Delta E_C$ (V)* | $P_r$ (μC/cm$^2$)* | $\Delta E_C$ (V)* |
| PVDF:CTFE (90/10) | 90:10 | 3.6 ± 0.5 | 51.1 | 4.2 ± 0.5 | 50.9 | 4.1 ± 0.5 | 50.7 |
| PVDF:CTFE (85/15) | 85:15 | 3.4 ± 0.5 | 47.2 | 3.6 ± 0.5 | 47.8 | 4.3 ± 0.5 | 48.3 |
| PVDF:CTFE (80/20) | 80:20 | 2.8 ± 0.5 | 46.4 | 3.0 ± 0.5 | 48.5 | 3.6 ± 0.5 | 48.7 |

* All ferroelectric properties are averaged out from 10 MFM cells.

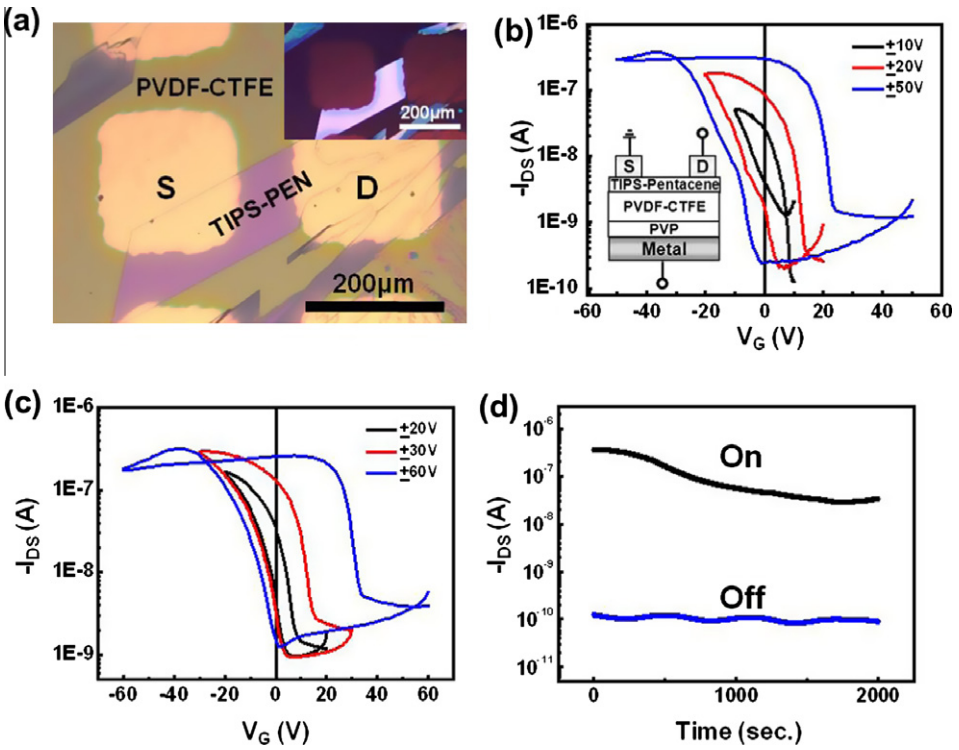


**Fig. 4.** (a) A bright field OM image of a top view of a bottom gate, top contact FeFET with single crystal TIPS-PEN solution-grown on a PVDF-CTFE 90/10 film surface. The inset of (a) is an OM image of the highly birefringent single crystalline TIPS-PEN under cross polarizers. $I_D$–$V_G$ transfer curves of single crystal TIPS-PEN FeFETs with PVDF-CTFE gate insulators (b) annealed at 130 °C for 2 h and (c) re-crystallized from molten state at 200 °C. The inset depicts the schematic of FeFET device structure. (d) Data retention performance of a single crystal TIPS-PEN FeFET memory with a ferroelectric PVDF-CTFE gate insulator annealed at 130 °C for 2 h. Both ON and OFF currents were detected at zero gate voltage with the continuous drain voltage of −5 V after single voltage pulse of −60 and +60 V for ON and OFF current, respectively.

A FeFET with a PVDF-CTFE 90/10 re-crystallized from the molten state also exhibits well saturated $I_{SD}$ hysteresis loops with gate voltage sweep as shown in Fig. 4c, similar to those obtained with the PVDF-CTFE consisting of β type crystals. Our results again confirm the ferroelectric PVDF-CTFE films independent of the types of crystals developed under the different thermal processing steps. Data retention is one of the most critical requirements for realizing a reliable non-volatile FeFET memory with a ferroelectric polymer. Data retention properties of both ON and OFF state of a single crystal TIPS-PEN FeFET device with a PVDF-CTFE 90/10 layer annealed at 130 °C were evaluated by independently measuring $I_{DS}$ in the ON and OFF state under zero gate bias with a constant $V_{DS}$ of −5 V after polarization switching at ±60 V. Fig. 4d shows the results from a 30 min retention measurement. Both ON and OFF current measurements, taken once per second, in spite of a slight decrease of ON current at the beginning of the measurement do not show significant changes over a 30 min time range. Extrapolation of both currents over time allows the estimation of long-time data retention capability of our device in excess of a few years as long as the single crystal TIPS-PEN is robust under environmental degradation. It should also noted that a FeFET with a PVDF-CTFE re-crystallized from the molten state also displayed a reliable data retention performance in which ON current initially decreased but remained constant for approximately 1 h measurement (Supporting information, S5).

The notable ferroelectric polarization of a PVDF-CTFE we observed at electric field above its coercive field regardless of the types of crystals can also guarantee high dielectric properties below its coercive field. In this sense, PVDF-CTFEs examined in the current work may be also applicable for organic field effect transistor (OTFT). In fact, the high

dielectric constant of approximately 12 in the frequency range of 1–100 kHz was reported in the literature [27] and thus a PVDF-CTFE can be employed as a dielectric layer of an OTFT for low voltage operation. In addition, considering that source-drain current hysteresis of an OTFT frequently appears at high gate voltage sweep and tends to increase with the sweep voltage, an OTFT containing a PVDF-CTFE with the high dielectric constant can significantly reduce the hysteresis. Furthermore, PVDF-CTFEs can be applied for temperature and pressure sensors based on the principles of pyro and piezoelectricity, respectively. Since many pryo and piezoelectric sensors of ferroelectric PVDF and PVDF-TrFEs in particular based on field effect transistor device architecture [41–43], ferroelectric PVDF-CTFEs investigated in the current work can be apparently employed as pressure as well as temperature sensing materials and it would be interesting to examine how pyro and piezoelectricity behaves in these materials.

## 4. Conclusions

We demonstrated the ferroelectric properties of PVDF-CTFE copolymers with various CTFE compositions prepared under different thermal processing steps in both MFM capacitors and FeFET memory elements. The characteristic $\alpha$ and $\beta$ type crystals of PVDF-CTFEs were developed with the unique chain conformations, crystallographic ordering and surface microstructures when the films were re-crystallized from the molten state and annealed at 130 °C, respectively. Both types of crystals turned out ferroelectric in PVDF-CTFE films, giving rise to saturated polarization and current hysteresis loops with $P_r$ of approximately 4 $\mu C/cm^2$ and with ON/OFF ratio of approximately $10^3$ in non-volatile MFM and FeFET memory elements, respectively. The reliable data retention properties of FeFETs containing PVDF-CTFE films treated with the different thermal processing steps confirmed non-volatile ferroelectric nature of both $\alpha$ and $\beta$ crystals, rendering those films suitable for thermal history independent non-volatile ferroelectric polymer memory.

## Acknowledgments

This work was supported by the Second Stage of the Brain Korea 21 Project in 2006 and by a National Research Foundation of Korea (NRF) Grant funded by the Ministry of Science and Technology (MEST), Republic of Korea (No. R11-2007-050-03001-0), (MOEHRD; KRF-2009-0080235). This research was also supported by the Converging Research Center Program through the Ministry of Education, Science and Technology (Nos. 2010K001430 and 2011K000685). The X-ray experiments at PAL (4C2 beamline), Korea were supported by MEST and POSCO, Korea.

## Appendix A. Supplementary data

Supplementary data associated with this article can be found, in the online version, at doi:10.1016/j.orgel.2011.11.018.

## References

[1] O. Auriello, J.F. Scott, R. Ramesh, Phys. Today 51 (1998) 22.
[2] S. Ducharme, T.J. Reece, C.M. Othon, R.K. Rannow, IEEE Trance. Device Mater. Reliab. 5 (2005) 720.
[3] R.C.G. Naber, C. Tanase, P.W.M. Blom, G.H. Gelinck, A.W. Marsman, F.J. Touwslager, S. Setayesh, D.M. de Leeuw, Nat. Mater. 4 (2005) 243.
[4] K. Omote, K. Koga, H. Ohigashi, J. Appl. Phys. 81 (1997) 2760.
[5] X. Zhao, V. Bharti, T. Romotowski, F. Tito, R. Ting, Q.M. Zhang, Appl. Phys. Lett. 73 (1998) 2054.
[6] T. Furukawa, IEEE Trans. Electr. Insul. 24 (1989) 375.
[7] H.L.W. Chan, Z. Zhao, K.W. Kwok, C. Alquie, C. Boue, J. Lewimer, C.L. Choy, J. Appl. Phys. 80 (1996) 3982.
[8] J.H. Mcfee, J.G. Bergman, G.R. Crane, Ferroelectrics 3 (1972) 305.
[9] G. Zhu, Y. Gu, H. Yu, S. Fu, Y. Jiang, J. Appl. Phys. 110 (2011) 024109.
[10] G.G. Lee, E. Tokumitsu, S.M. Yoon, Y. Fujisaki, J.W. Yoon, H. Ishiwara, Appl. Phys. Lett. 99 (2011) 012901.
[11] J. Hoffman, X. Pan, J.W. Reiner, F.J. Walker, J.P. Han, C.H. Ahn, T.P. Ma, Adv. Mater. 22 (2010) 2957.
[12] R.C.G. Naber, K. Asadi, P.W.M. Blom, D.M. de Leeuw, B.B. de Boer, Adv. Mater. 22 (2010) 933.
[13] Y.J. Shin, S.J. Kang, H.J. Jung, Y.J. Park, I. Bae, D.H. Choi, C. Park, ACS Appl. Mater. Interfaces 3 (2011) 582.
[14] J. Chang, C.H. Shin, Y.J. Park, S.J. Kang, H.J. Jeong, K.J. Kim, C.J. Hawker, T.P. Russell, D.Y. Ryu, C. Park, Org. Electron. 10 (2009) 849.
[15] J. Chang, H.J. Jung, H. Jeong, Y.J. Park, J. Sung, S.J. Kang, G.Y. Jung, M.M. Sung, C. Park, Org. Electron. 12 (2011) 98.
[16] T. Furukawa, Y. Takahashi, T. Nakajima, Curr. Appl. Phys. 10 (2010) e62.
[17] J.C. Scott, L.D. Bozano, Adv. Mater. 19 (2007) 1452.
[18] S.J. Kang, I. Bae, Y.J. Shin, Y.J. Park, J. Huh, S. Park, H. Kim, C. Park, Nano Lett 11 (2011) 138.
[19] T.J. Reece, S. Ducharme, A.V. Sorokin, M. Poulsen, Appl. Phys. Lett. 82 (2003) 142.
[20] A.J. Lovinger, Science 220 (1983) 1115.
[21] J.B. Lando, H.G. Olf, A. Peterlin, J. Polym. Sci., Part A-1: Polym. Chem 4 (1966) 941.
[22] J.P. Luongo, J. Polym. Sci., Part A-2: Polym. Phys. 10 (1972) 1119.
[23] K. Matsushige, T. Takemura, J. Polym. Sci., Polym. Phys. Ed. 16 (1978) 921.
[24] Y.J. Park, S.J. Kang, H.S. Lee, M.S. Lee, U. Chung, I.J. Park, C. Park, Appl. Phys. Lett. 88 (2006) 242908.
[25] L. Zhang, S. Ducharme, J. Li, Appl. Phys. Lett. 91 (2007) 172906.
[26] B. Chu, X. Zhou, B. Neese, Q.M. Zhang, F. Bauer, IEEE Trans. Dielect. Electr. Insul. 13 (2006) 1162.
[27] X. Zhou, B. Chu, B. Neese, M. Lin, Q.M. Zhang, IEEE Trans. Dielect. Electr. Insul. 14 (2007) 1133.
[28] X. Zhou, Q. Chen, Q.M. Zhang, S. Zhang, IEEE Trans. Dielect. Electr. Insul. 18 (2011) 463.
[29] F. Guan, Z. Yuan, E.W. Shu, L. Zhu, Appl. Phys. Lett. 94 (2009) 052907.
[30] W. Xia, Z. Xu, F. Wen, W. Li, Z. Zhang, Appl. Phys. Lett. 97 (2010) 222905.
[31] B. Chu, X. Zhou, K. Ren, B. Neese, M. Lin, Q. Wang, F. Bauer, Q.M. Zhang, Science 313 (2006) 334.
[32] I. Bae, S.J. Kang, Y.J. Shin, Y.J. Park, R.H. Kim, F. Mathevet, C. Park, Adv. Mater. 23 (2011) 3398.
[33] M. Benz, W.B. Euler, O.J. Gerory, Macromolecules 35 (2002) 2682.
[34] R. Gregorio, N.C.P. de Souza Nociti, J. Phys. D. 28 (1995) 432.
[35] K. Tashiro, M. Kobayashi, H. Tadokoro, Macromolecules 14 (1981) 1757.
[36] K. Tashiro, Y. Itoh, M. Kobayashi, H. Tadokoro, Macromolecules 18 (1985) 2600.
[37] A.K. Dikishit, A.K. Nandi, Macromolecules 33 (2000) 2616.
[38] S.J. Kang, Y.J. Park, J. Sung, P.S. Jo, K.J. Kim, B.O. Cho, C. Park, Appl. Phys. Lett. 92 (2008) 012921.
[39] S.J. Kang, I. Bae, J.-H. Choi, Y.J. Park, P.S. Jo, Y. Kim, K.J. Kim, J.-M. Myoung, E. Kim, C. Park, J. Mater. Chem. 21 (2011) 3619.
[40] Y.J. Park, I.-S. Bae, S.J. Kang, J. Chang, C. Park, IEEE Trans. Dielectr. Electr. Insul. 17 (2010) 1135.
[41] M. Zirkl, A. Haase, A. Fian, H. Schon, C. Sommer, G. Jakopic, G. Leising, B. Stadlober, I. Graz, N. Gaar, R. Schwodiauer, S. Bauer-Gogonea, S. Bauer, Adv. Mater. 19 (2007) 2241.
[42] I. Graz, M. Krause, S. Bauer-Gogonea, S. Bauer, S.P. Lacour, B. Ploss, M. Zirkl, B. Stadlober, S. Wagner, J. Appl. Phys. 106 (2009) 034503.
[43] I. Graz, M. Kaltenbrunner, C. Keplinger, R. Schwodiauer, S. Bauer, S.P. Lacour, S. Wagner, Appl. Phys. Lett. 89 (2006) 073501.